This paper has been presented at IEEE ICC 2019.

Hidden Markov Model based Machine Learning for mMTC Device Cell Association in 5G Networks

Indika A. M. Balapuwaduge and Frank Y. Li
Dept. of Information and Communication Technology, University of Agder (UiA), N-4898 Grimstad, Norway
Email: {indika.balapuwaduge; frank.li}@uia.no

***Abstract*—Massive machine-type communication (mMTC) is expected to play a pivotal role in emerging 5G networks. Considering the dense deployment of small cells and the existence of heterogeneous cells, an MTC device can discover multiple cells for association. Under traditional cell association mechanisms, MTC devices are typically associated with an eNodeB with highest signal strength. However, the selected eNodeB may not be able to handle mMTC requests due to network congestion and overload. Therefore, reliable cell association would provide a smarter solution to facilitate mMTC connections. To enable such a solution, a hidden Markov model (HMM) based machine learning (ML) technique is proposed in this paper to perform optimal cell association. As such, we consider MTC devices with network-assisted decision-making capabilities for selecting the most appropriate eNodeB for data transmission. The proposed HMM based ML technique focuses mainly on the reliability and availability of network resources. Correspondingly, two schemes are developed based on the classical reliability function and the next probable state of the HMM. Based on simulations under various configurations, we demonstrate the advantage of the proposed schemes over a random cell selection scheme.**

I. Introduction

Upcoming 5G mobile and wireless networks provide significant advancements in three broad categories, namely enhanced mobile broadband (eMBB), massive machine-type communications (mMTC), and ultra-reliable and low latency communications (URLLC). Due to a massive number of devices, high-density deployment, small-sized packet transmissions, and a large uplink-to-downlink traffic volume ratio, providing mMTC services appears as a challenging task in 5G. For instance, one of the essential requirements for mMTC applications is high *availability and reliability* to ensure low latency, accurate, and flawless operations.

To provide mMTC services, multiple technical challenges need to be addressed. Those challenges include quality of service (QoS) provisioning, radio access network (RAN) congestion control for dynamic and sporadic MTC traffic [1]. On the other hand, dealing with huge signaling overhead generated by a massive number of autonomous connections is another tedious and resource-demanding task. Fig. 1 illustrates a prospective network architecture for MTC applications where a heterogeneous network (HetNet) consisting of multiple small cells is deployed in an area of interest [2] [3]. These cells are overlapped in design to prevent blind spots and achieve seamless handover. In LTE-A, the co-existence of heterogeneous cells (including relays, picocells, and femtocells) is expected in order to provide better coverage and capacity. Moreover, network slicing is recognized as a promising technology in

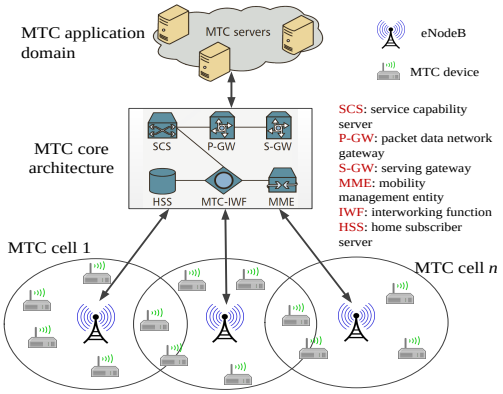

Fig. 1. An envisioned MTC architecture by 3GPP [4].

mMTC to create multiple end-to-end virtual networks over a common infrastructure [5]. Consequently, MTC devices should be able to dynamically select an appropriate cell for association to fit the MTC requirements since they may be covered by multiple cells.

In a heterogeneous network with overlapping cells, cell association could be a critical decision for MTC performance considering the needed radio resources during and after the cell selection process. In such scenarios, MTC devices are expected to select the most appropriate eNB without calling the expensive core network functions based on the instantaneous value of the received signal strength, e.g., reference signal received quality (RSRQ) [6] or access barring information received via system information blocks (SIBs) [7]. Therefore, MTC devices need to be designed with decision making capability to select the target eNB in a network assisted manner. This also leads to a considerable reduction of overhead traffic. However, due to a massive number of low power and low complex devices and heavy burst, MTC devices are not able to estimate accurately the random access intensity or load condition of each eNB [8]. In an overload condition, random access attempts can be rejected frequently by the eNB. Correspondingly, it has become an interesting issue to analyze how MTC devices are aware of the ongoing status of each eNB in order to perform an effective cell association.

In [9], a cell association scheme is proposed for small cell networks by considering load balancing to optimize the base station (BS) idle time. In another study, [10], a cell association scheme is designed for HetNets based on joint consideration of the signal-to-interference-plus-noise ratio (SINR) and the

traffic load of the BS. Moreover, [11] investigates effective cell association for load balancing in HetNets. However, those approaches do not consider cell association for MTC scenarios in 5G networks. This paper proposes an HMM based machine learning (ML) algorithm with two cell association schemes to let MTC devices select an appropriate cell among the available cell set. The proposed ML algorithm runs on MTC devices and enables the devices to select the eNB intelligently, hence aiming at mitigating signaling overhead in random access and thus achieving better performance.

The remainder of this paper is structured as follows. The network scenario and the discrete time Markov chain (DTMC) model are described in Sec. II. The HMM problems and solutions are outlined in Sec. III. Thereafter Sec. IV describes the proposed cell association schemes based on our network scenario. The simulation results are provided in Sec. V. Finally, we conclude this paper in Sec. VI.

II. Network Scenario and DTMC Model

This section presents the adopted network scenario and assumptions, and then the underlying DTMC model is described.

A. Network Scenario and Assumptions

Consider a RAN with N cells and that each cell consists of a single eNB. Let Z be the number of resources available at each eNB for admitting users. These resources can represent preambles, resource blocks (RBs), or simply channels. Although a huge number of MTC devices are connected to a given eNB, only a subset of them becomes active and attempts to send their data at a given time following a random arrival distribution, for instance, Poisson or Beta distribution.

As illustrated in Fig. 1, an MTC device can be covered by more than one eNB. According to the basic positioning support introduced in 3GPP Release 13, RSRQ is available for devices [12]. This information will be transformed into an observation output which is detected by a device. In this study, we consider a time-slotted structure where the time slots are indicated as $t \in \{1, 2, \cdots, T\}$ such that an active device detects one observation output at each time slot.

B. eNB Status and DTMC Modeling

In this study, we model the status of each eNB by a set $\mathcal{S} = \{y_1, y_2\}$ where y_1 represents that eNB can accommodate resources (preambles, RBs, or channels) to an MTC device and y_2 indicates that eNB blocks communication requests from MTC devices due to insufficient resources. In other words, when the status of an eNB is y_2, all Z resources are occupied or not allocatable to devices. Then, by assuming the memoryless property, a general state of the corresponding first-order DTMC can be represented as $\boldsymbol{x} = \{x_1, x_2, \cdots, x_N\}$ where $x_i \in (y_1, y_2)$ denotes the channel occupancy status of the i^{th} cell. Therefore the total number of states in this system becomes 2^N. Moreover, the states are denoted as $1, 2, 3, \cdots, i, \cdots, 2^N$ and i is simply the i^{th} state. Note however that *the DTMC is not observable by MTC devices*. Instead, only the observation output is detected at each time slot. That is, the state transition probabilities and observation probabilities are hidden to the devices.

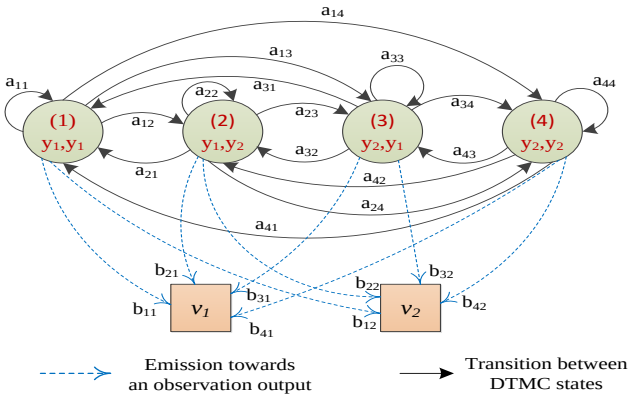

Fig. 2. A DTMC model for a 2 cell scenario. Each cell can be in one of the two modes, i.e., $\{y_1, y_2\}$. The observation outputs are denoted as v_1 and v_2. The dashed lines indicate the observation probabilities of each state towards the two observation outputs.

As an example, the corresponding DTMC of the HMM when $N = 2$ is illustrated in Fig. 2. Herein, a_{ij} denotes the transition probability from state i to state j. Denote by $\boldsymbol{A}$ the state transition matrix. $\boldsymbol{A}$ contains the probability that a hidden state will evolve to another state, given the current state. Moreover, denote the system state at time slot t as S_t. An initial state probability value which indicates how likely it is for an input measure to start in state i is given as $\pi_i = P(S_0 = i)$.

Without knowing the cell status of eNBs, MTC devices are not able to select their eNB properly. Therefore, in order to solve this problem, we can apply an *unsupervised machine learning* technique. Therein, HMM has shown better results in earlier studies due to its capability of modeling sequential data. In the next section, we present the mathematical structure of the HMM as the required preliminaries for proposing ML based cell association schemes.

III. Cell Association Preliminaries: HMM based Machine Learning

Assume that each MTC device obtains an observation output o_t at every time slot t. The observation output sequence during period $(0, T]$ is represented as $\boldsymbol{O^T} = \{o_1, o_2, \cdots, o_T\}$. Let $\boldsymbol{V} = \{v_1, v_2, \cdots, v_L\}$ be the set of possible observations. The probability of observing the output v_k, $k \in (1, 2, \cdots L)$ at time slot t given that the system is in state j, $j \in (1, 2, \cdots, 2^N)$ is denoted as $b_j(v_k)$, i.e., $b_j(v_k) = P(o_t = v_k | S_t = j)$. For instance, in Fig. 2 and also in our simulations, each hidden state of the DTMC model contributes to two possible outputs, denoted as v_1 and v_2. Let $\boldsymbol{B} = \{b_j(v_k)\}$ be the observation probability matrix of the HMM. Correspondingly, $\boldsymbol{B}$ contains the probability that a particular measurable output can be observed, provided that the model is in one of the hidden states. After all these notations, the HMM can be denoted in a compact form as $\lambda = (\boldsymbol{A}, \boldsymbol{B}, \boldsymbol{\pi_0})$ where $\boldsymbol{\pi_0}$ is the initial probability distribution of DTMC states, i.e., $\boldsymbol{\pi_0} = \{\pi_1, \pi_2, \cdots, \pi_{2^N}\}$. To perform the proposed cell association, we need to solve the following three problems first.

A. HMM Evaluation Problem

The first problem is to determine the probability of the observed sequence $\boldsymbol{O^T}$ given the DTMC model $\lambda' = (\boldsymbol{A'}, \boldsymbol{B'}, \boldsymbol{\pi'_0})$ where $\boldsymbol{A'}, \boldsymbol{B'}$, and $\boldsymbol{\pi'_0}$ denote the initial estimation of the state transition matrix, observation probability matrix, and the probability distribution of DTMC states respectively. To do so, we define a *forward variable* $\alpha_t(i)$ as the probability of the partial observation sequence up to time t and state i at time t. According to the initial conditions, we can state that $\alpha_j(1) = \pi_j b_j(o_1),\ \forall j$. To recursively calculate $\alpha_j(t),\ j = 1, 2, \cdots, 2^N$ through dynamic programing, we can use the above initial condition and the following equation

$$\alpha_j(t+1) = b_j(o_{t+1}) \sum_{i=1}^{2^N} \alpha_i(t) \times a_{ij}.$$

Then, the probability of the observation sequence, $\boldsymbol{O^T}$, when the model λ' is given, can be expressed as

$$P(\boldsymbol{O^T}|\lambda') = \sum_{i=1}^{2^N} \alpha_i(T). \tag{1}$$

The above expression will be applied in our proposed ML procedure to check the accuracy of the obtained decision.

B. HMM Decoding Problem

In the second problem, we can find the most likely sequence of the hidden states which could have generated a given output sequence. Unlike in the evaluation problem, herein, we need to define an *optimality criterion*. Without loss of generality, the states which are individually most likely at each time slot are considered. Denote the probability of being in state i at time t, given the model λ' as $\gamma_t(i)$. We have $\gamma_t(i) = P(S_t = i|\boldsymbol{O^T}, \lambda')$. To compute this, we need a *backward variable*, $\beta_t(i)$, i.e., the probability of the partial observation sequence from $t+1$ to the end, given state i at time t. Initially, $\beta_T(i) = 1,\ \forall i$. Similar to the forward variable calculation, the following recursion needs be used to compute the backward variable

$$\beta_t(i) = \sum_{j=1}^{2^N} a_{ij} b_j(o_{t+1}) \beta_{t+1}(j).$$

Correspondingly,

$$\gamma_t(i) = \frac{\alpha_t(i)\beta_t(i)}{\sum_{i=1}^{2^N} \alpha_t(i)\beta_t(i)}. \tag{2}$$

Once we know the likelihood of all states being at time t, the individually most likely state at time t becomes

$$w_t = \underset{1 \le i \le N}{\operatorname{argmax}}\ \gamma_t(i). \tag{3}$$

C. HMM Learning Problem

In this final problem, the model parameters, i.e., $\boldsymbol{A}, \boldsymbol{B}$, and $\boldsymbol{\pi_0}$ need to be accurately estimated from the observation sequence assuming that N and L are known parameters. With the recent advances in ML, there exist several techniques to solve this type of parameter estimation problems based on both supervised and unsupervised learning. However, it is infeasible to solve this hidden state problem by supervised learning since the observation sequence cannot be used to generate any outcome. On the other hand, unsupervised ML techniques can provide a promising solution to this problem. To do so, the HMM needs to be trained in order to estimate the hidden model. In this paper, we adopt the training process proposed in [13] by utilizing the well-known Baum-Welch algorithm. It is worth mentioning that this algorithm consumes a short time period (in our simulations less than 1 second to generate converged parameters within 100-400 training rounds). Therefore, high power consumption is not required for MTC devices.

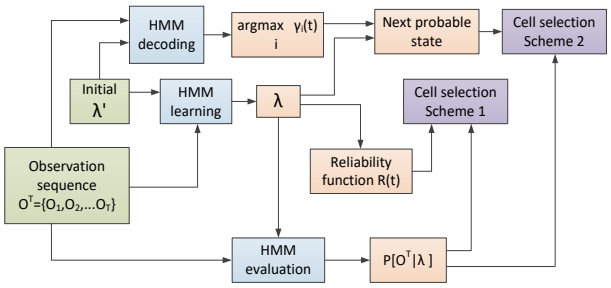

Fig. 3. The relationship between the proposed cell association schemes and the hidden Markov model. The initially assumed HMM is denoted as λ'.

IV. Proposed Cell Association Schemes

The schematic diagram of the main components of the proposed HMM based ML algorithm is illustrated in Fig. 3. For cell association, two schemes are proposed in Algorithm 1 in which an MTC device can select one of the two schemes. In this algorithm, Lines 1-5 indicate the collection of observation outputs at each time step by an MTC device. Line 6 extracts the required observation sequence, $\boldsymbol{O^T}$, upon the MTC request. Based on this and the other input parameters, Lines 7 and 8 estimate the model parameters by using the HMM learning process. The accuracy of the output parameters is checked in Line 9 by computing the likelihood of the observation sequence. If the likelihood value is sufficiently greater than a predefined value, P_{th}, the algorithm can proceed. Otherwise, the MTC device is advised to restart the algorithm with another observation sequence or go for random cell selection as indicated in Lines 10-15. Lines 16-27 and Lines 28-40 correspond to Scheme 1 and Scheme 2 described in the next two subsections respectively.

A. Scheme 1: Reliability Function based Cell Association

In this scheme, we define a reliability function based on the classical dependability theory. First we use T_i to denote the number of time steps spent at state i when it is visited. This is a discrete random variable (RV) which has a geometric distribution with parameter a_{ii}. Therefore, the distribution of the state holding time T_i is geometric with parameter a_{ii} as $P(T_i = n) = (1 - a_{ii})(a_{ii})^{n-1}$. Based on this, we obtain

$$\begin{aligned} P(T_i \le n) &= \sum_{k=1}^{n} P(T_i = k), \\ &= (1 - a_{ii})[1 + a_{ii} + \cdots + {a_{ii}}^{n-1}] = 1 - {a_{ii}}^n. \end{aligned} \tag{4}$$

Algorithm 1: HMM based ML algorithm for cell association in MTC following the reliability function $R(t)$ and the next probable state for Scheme 1 and Scheme 2 respectively.

Input: $\lambda' = ((\boldsymbol{A'}, \boldsymbol{B'}, \boldsymbol{\pi'_0})$: Initial HMM
Input: N : Total number of states in the HMM
Input: T : Length of the required observation sequence
Output: W : The selected cell for channel access
[1] Device requests MTC at time step n
[2] Observation output at time step l is $Obs(l)$
[3] **for** $l = 1 : 1 : n$ **do**
[4] | $o_l = Obs(l)$
[5] **end**
[6] $\boldsymbol{O^T} = \{o_{n-(T-1)}, o_{n-(T-2)}, \cdots, o_{n-1}, o_n\}$
[7] Run HMM Learning algorithm with the inputs λ' and $\boldsymbol{O^T}$
[8] Calculate $\lambda = (\boldsymbol{A}, \boldsymbol{B}, \boldsymbol{\pi_0})$
[9] Evaluate $P(O^T|\lambda)$ via HMM evaluation
[10] **if** $P(O^T|\lambda) > P_{th}$ **then**
[11] | Follow the rest of the procedure from Line **[16]**
[12] | **else**
[13] | | Restart the algorithm with another observation sequence
[14] | | or go for random cell selection
[15] | **end**
[16] **end**
[17] **if** *Scheme 1 is selected* **then**
[18] | Select $K = \underset{i}{\operatorname{argmax}}\ a_{ii}$
[19] | Consider K^{th} state for the following code:
[20] | **if** $\exists j : x_j = y_1,\ j \leq N$ **then**
[21] | | Select cell W where $W = min\{W|x_W = y_1, W \leq N\}$
[22] | | **else**
[23] | | | Select $K' = \underset{i,\ i \neq K}{\operatorname{argmax}}\ a_{ii}$
[24] | | | Consider $(K')^{th}$ state for the following code:
[25] | | | Select cell W where $W = min\{W|x_W = y_1\}$
[26] | | **end**
[27] | **end**
[28] **end**
[29] **if** *Scheme 2 is selected* **then**
[30] | Calculate $\boldsymbol{\pi}(T) = \boldsymbol{\pi}_0 \boldsymbol{A}^T = \{\boldsymbol{\pi}_T^1, \boldsymbol{\pi}_T^2, \cdots, \boldsymbol{\pi}_T^{2^n}\}$ where $\boldsymbol{\pi}_T^i = P(S_T = i)$
[31] | Select $K = \underset{i}{\operatorname{argmax}}\ \boldsymbol{\pi}_T^i$
[32] | Consider K^{th} state for the following code:
[33] | **if** $\exists j : x_j = y_1,\ j \leq N$ **then**
[34] | | Select cell W where $W = min\{W|x_W = y_1, W \leq N\}$
[35] | | **else**
[36] | | | Select $K' = \underset{i,\ i \neq K}{\operatorname{argmax}}\ \boldsymbol{\pi}_T^i$
[37] | | | Consider $(K')^{th}$ state for the following code:
[38] | | | Select cell W where $W = min\{W|x_W = y_1\}$
[39] | | **end**
[40] | **end**
[41] **end**

Consequently, the probability that the number of time steps spent at state i is greater than n can be derived as

$$P(T_i > n) = 1 - P(T_i \leq n) = {a_{ii}}^n. \tag{5}$$

This is equal to the n^{th} power of the transition probability to the state itself. In dependability analysis, the reliability function is analytically related to the probability of success time and it is defined as $R(t) = P(T > t)$ where $t > 0$ and T is the RV representing time to failure. Therefore the expression derived in (5) is corresponding to the reliability function, i.e., $R(t) = P(T_i > t) = {a_{ii}}^t$. This result is adopted when selecting the most *reliable* cell in Scheme 1.

Therein, the state which has the maximum self-transition probability is selected in Line 17. Line 19 checks whether the selected state has at least one cell with an idle channel. If not, from Line 22, the state which has the second maximum self-transition probability will be selected. The algorithm does not need to go for a third maximum self-transition probability calculation since in our system model, there exists only a single state which has the condition of all occupied cells. The statements in Line 20 and Line 24 suggest the appropriate cell for starting the requested MTC.

B. Scheme 2: Next Probable State based Cell Association

Instead of selecting the state at which channel availability continues for the next n time slots as in Scheme 1, Scheme 2 checks only the most probable state at the next time slot. Therefore, availability is considered as having high priority than reliability. The corresponding selection procedure is explained in Algorithm 1 from Line 28.

In this scheme, we perform a transient analysis of the DTMC. The main tool for transient analysis is provided by the recursive relation $\boldsymbol{\pi}(t+1) = \boldsymbol{\pi}(t)\boldsymbol{A}$ where $\boldsymbol{\pi}(t)$ denotes the state probability vector at time t. We can express this relationship in terms of a given initial state probability vector $\boldsymbol{\pi}(0)$ as $\boldsymbol{\pi}(t) = \boldsymbol{\pi}(0)\boldsymbol{A}^t,\ t = 1, 2, \cdots$. Using this result, we obtain the state probability vector of the solved HMM after T time steps as noted in Line 29. Then the state which has the maximum probability of becoming the next state is selected in Line 30. The rest of the code follows a similar procedure as mentioned in Scheme 1.

To calculate the state probability vector in Line 29, we can also adopt an alternative method based on the HMM decoding output as illustrated in Fig. 3 instead of the aforementioned one. Therein, the state probability vectors corresponding to the most probable state sequence can be obtained. Then, $\boldsymbol{\pi}(T) = \boldsymbol{\pi}(T-1)\boldsymbol{A}$ can be calculated in Line 29. In simulations, we adopt $\boldsymbol{\pi}(T) = \boldsymbol{\pi}_0\boldsymbol{A}^T$ to evaluate the performance of Scheme 2.

V. Simulation Results and Discussions

In this section, we provide comprehensive simulations to illustrate the performance of the proposed schemes.

A. Network Scenario Setup and Simulation Procedure

Consider a network with $N = 2$ cells similar to the scenario presented in Fig. 2. For the sake of simplicity, we consider channels as the required resources in an MTC network. Furthermore, we assume that each cell consists of $Z = 2$ channels. A cell is said to be in mode y_2 if both channels are occupied and in mode y_1 if there is at least one available channel. At each time slot, an MTC device observes an output, either v_1 or v_2. Note that v_1 and v_2 indicate the signs of the channel available and unavailable conditions respectively.

Upon an MTC request, the device runs the proposed HMM based ML algorithm by admitting its observation sequence of length $T = 4$ and the initial model λ'. Correspondingly, the states of the HMM become $\{(y_1, y_1), (y_1, y_2), (y_2, y_1), (y_2, y_2)\}$ where the first and the second elements of each state are representing the mode of Cell 1 and Cell 2 respectively. The elements of the initial

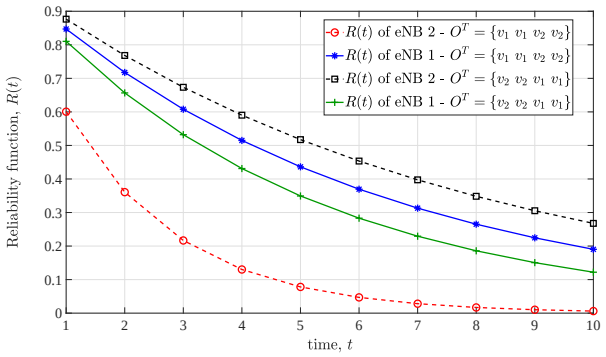

Fig. 4. Reliability function with respect to different observation sequences. The solid and dashed lines indicate $R(t)$ of eNB 1 and eNB 2 respectively.

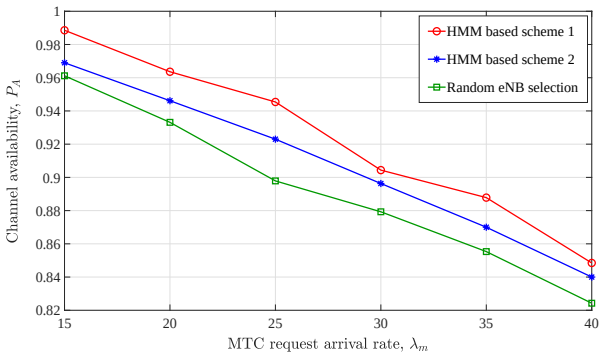

Fig. 5. Channel availability as the MTC device arrival rate varies when the arrival distribution follows a Poisson process.

state transition probability matrix $\boldsymbol{A'}$ and the observation probability matrix $\boldsymbol{B'}$ can be selected randomly since the initial estimation of them is not much critical on the final output. However, each row sum of $\boldsymbol{A'}$ and the column sum of $\boldsymbol{B'}$ should be equal to 1. Furthermore, we assume that the system's initial state is (y_1, y_1). Therefore $\boldsymbol{\pi'_0} = \{1, 0, 0, 0\}$.

In our simulations, we consider up to 20k MTC devices and MTC arrivals are modeled either as a Poisson process with rate λ_m or as a Beta distribution with two shape parameters α, β. Beta distribution is one of the proposed traffic models for MTC arrivals by 3GPP [14] since it precisely captures the burstiness of MTC traffic. On the other hand, when MTC devices do not follow a synchronized access, MTC arrivals can be modeled as a Poisson process. In both cases, the admitted service stays in the system for a random amount of duration that follows exponential distribution with mean $1/\mu$. During the simulation period, the arrivals and completions of MTC services are checked, processed, and tracked. At the end of each simulation, the statistics of the system are calculated. For example, blocking probability, P_B, is obtained based on the number of blocked MTC requests divided by the total number of MTC requests during the simulation period.

In order to generate the observation sequence at an MTC request, we adopt the following approach. First the set of feasible observation sequences of length T is obtained. For instance, when $T = 2$ and $L = 2$, we have four possible observation sequences as $seq_1 = \{v_1, v_1\}$, $seq_2 = \{v_1, v_2\}$, $seq_3 = \{v_2, v_1\}$, and $seq_4 = \{v_2, v_2\}$. Therein, output v_1 indicates a sign of *channel available* condition while output v_2 indicates a sign of *channel unavailable* condition. For simulations, the observation sequences are randomly selected by considering the channel occupancy status. For instance, if all channels are available in the system at time t, seq_4 is not selected as the observation sequence of the MTC device at time t since it implies the occupied status of all channels.

B. Reliability Function of eNBs in Scheme 1

In Fig. 4, the impact of observation sequence on reliability function of eNBs is studied. Consider two possible observation sequences given by $seq_1 = \{v_1, v_1, v_2, v_2\}$ and $seq_2 = \{v_2, v_2, v_1, v_1\}$. As shown in the figure, if an MTC device receives seq_1, the reliability function value of the eNB 1 is higher than that of eNB 2. In other words, the chance of acquiring a vacant channel during the next $t > 0$ slots is higher in eNB 1. Therefore, with this observation sequence, the MTC device which employs Scheme 1 selects eNB 1. However, for seq_2, eNB 2 shows higher reliability than eNB 1. This difference can be expected since the two sequences are complement to each other. Note that the reliability function always monotonically decreases, i.e., $R(u) \leq R(v)\ \forall\ u > v$.

C. Channel Availability

In this paper, channel availability, P_A, is calculated as $1 - P_B$, i.e., the fraction of MTC requests which received channel access with respect to the total number of requests. We study the impact of the MTC arrival rate on channel availability in Fig. 5 based on a Poisson process. As illustrated in this figure, when we increase the arrival rate, the channel availability decreases. Clearly, the more the MTC requests in the unit time, the higher the possibility that an MTC request is blocked due to a fixed amount of resources (channels). The most evident observation we can make from this figure is that the proposed two schemes outperform the random cell selection scheme. In the random scheme, MTC devices arbitrarily select one of the available eNBs for communication regardless of the observation sequence. In Scheme 1, however, MTC devices search for the most reliable cell based on the reliability function estimated after the HMM learning process. On the other hand, MTC devices which adopt Scheme 2 search for the most available cell based on the next probable state estimated after HMM learning. Therefore, both schemes lead to higher availability compared to the random cell selection.

In addition, it can be observed in Fig. 5 that Scheme 1 outperforms Scheme 2 in terms of channel availability. The reason can be explained as follows. Scheme 1 employs the reliability function as the main criterion for cell selection. Thus, in cell association, Scheme 1 checks the availability of channels for the next set of time slots. Instead of this reliability check, Scheme 2 evaluates only the next probable state to decide the appropriate cell. Therefore, the available time of idle channels is relatively higher in Scheme 1. Consequently, the probability of blocking an MTC device by the selected cell can be reduced in Scheme 1 compared to Scheme 2.

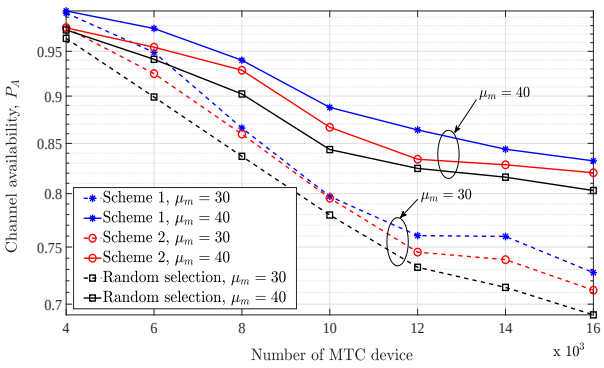

Fig. 6. Effects of the number of MTC devices on the channel availability when the arrival pattern follows Beta distribution.

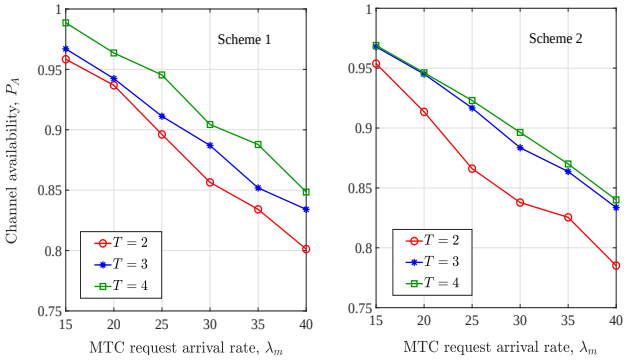

Fig. 7. Impact of the length of observation sequence on the performance of proposed two schemes.

D. MTC Arrivals under Beta Distribution

Fig. 6 demonstrates the results corresponding to the Beta distribution given by $Beta(\alpha, \beta)$. Herein, we select a 3GPP recommended model, $Beta(3, 4)$, to represent bursty traffic conditions [14]. In order to model synchronized arrival patterns, we need to keep $\alpha < \beta$ [15]. The first observation we can draw from this figure is that the increase in the number of MTC devices has a negative impact on channel availability. A larger MTC population will lead to a higher number of access requests and correspondingly a higher blocking probability since the amount of resources is fixed. On the other hand, increasing the service rate of MTC connections reduces the blocking probability of new requests since a large number of MTC requests can be completed within a time unit as illustrated in Fig. 6. Again, it is evident that the proposed cell selection schemes perform better than the random selection when MTC traffic is bursty.

E. Impact of the Observation Sequence Length

As already presented, the output of the ML algorithm highly depends on the observation sequence. Furthermore, Fig. 7 shows the impact of the observation sequence length, i.e., T time slots, on the performance of the two schemes. It can be observed that the highest channel availability of the MTC network is achieved when $T = 4$. When MTC devices select a short sequence (e.g., $T = 2$), the HMM may not be able to predict the actual channel condition accurately. Therefore, in order to improve the performance of the proposed schemes, an observation sequence with a sufficient length is required. To follow this point, an accuracy check is performed in Line 10 of Algorithm 1.

VI. Conclusions

This paper addresses the problem of optimal cell association in MTC networks through a network assisted decision making procedure. Accordingly, an HMM based machine learning technique is proposed together with two cell selection schemes. The proposed algorithm can be applied to MTC networks where devices can observe a sequence of symbols corresponding to the hidden states of the system. Based on this observation sequence, the proposed algorithm determines the most appropriate cell for association. Simulation results demonstrate that our schemes improve the network performance in terms of channel availability since it takes both availability and reliability of channels into account. In the simulations, both Poisson and Beta arrival distributions are applied to evaluate the performance under different MTC traffic conditions.

References

[1] P. Sarigiannidis, T. Zygiridis, A. Sarigiannidis, T. D. Lagkas, M. Obaidat, and N. Kantartzis, "Connectivity and coverage in machine-type communications," in *Proc. IEEE ICC*, May 2017, pp. 1–6.

[2] H. Shariatmadari, R. Ratasuk, S. Iraji, A. Laya, T. Taleb, R. Jäntti, and A. Ghosh, "Machine-type communications: Current status and future perspectives toward 5G systems," *IEEE Commun. Mag.*, vol. 53, no. 9, pp. 10–17, Sep. 2015.

[3] V. Capdevielle, A. Feki, and E. Sorsy, "Joint interference management and handover optimization in LTE small cells network," in *Proc. IEEE ICC*, Jun. 2012, pp. 6769–6773.

[4] 3GPP TS 23.682, "Architecture enhancements to facilitate communications with packet data networks and applications," v13.5.0, Mar. 2016.

[5] A. Baumgartner, T. Bauschert, F. D'Andreagiovanni, and V. S. Reddy, "Towards robust network slice design under correlated demand uncertainties," in *Proc. IEEE ICC*, May 2018, pp. 1–7.

[6] S. Dawaliby, A. Bradai, and Y. Pousset, "In depth performance evaluation of LTE-M for M2M communications," in *Proc. IEEE WiMob*, Oct. 2016, pp. 1–8.

[7] I. Leyva-Mayorga, L. Tello-Oquendo, V. Pla, J. Martinez-Bauset, and V. Casares-Giner, "Performance analysis of access class barring for handling massive M2M traffic in LTE-A networks," in *Proc. IEEE ICC*, May 2016, pp. 1–6.

[8] C. Chang, J. Chen, C. Chen, and R. Jan, "Scattering random-access intensity in LTE machine-to-machine (M2M) communications," in *Proc. IEEE GLOBECOM*, Dec. 2013, pp. 4729–4734.

[9] Y. Wang, S. Chen, H. Ji, and H. Zhang, "Load-aware dynamic biasing cell association in small cell networks," in *Proc. IEEE ICC*, Jun. 2014, pp. 2684–2689.

[10] B. Yang, G. Mao, X. Ge, and T. Han, "A new cell association scheme in heterogeneous networks," in *Proc. IEEE ICC*, Jun. 2015, pp. 5627–5632.

[11] H. Du, Y. Zhou, L. Tian, X. Wang, Z. Pan, J. Shi, and Y. Yuan, "A load fairness aware cell association for centralized heterogeneous networks," in *Proc. IEEE ICC*, Jun. 2015, pp. 2178–2183.

[12] 3GPP TS 36.305, "Stage 2 functional specification of user equipment (UE) positioning in E-UTRAN," v13.0.0, Dec. 2015.

[13] L. R. Rabiner, "A tutorial on hidden Markov models and selected applications in speech recognition," *IEEE Proc.*, vol. 77, no. 2, pp. 257–286, Feb. 1989.

[14] 3GPP TR 37.868, "Study on RAN improvements for machine-type communications," v11.0.0, Sep. 2011.

[15] X. Jian, X. Zeng, Y. Jia, L. Zhang, and Y. He, "Beta/M/1 model for machine type communication," *IEEE Commun. Lett.*, vol. 17, no. 3, pp. 584–587, Mar. 2013.